aELECTRONIC SUPPLEMENTARY INFORMATION

Lithiophilic/Lithiophobic ternary alloy anode with Ag concentration gradients guides uniform Li deposition

Yulu Liu[a], Qingwen Li[a], Qiushi Yao[b], Xianji Zhou[b], Wenwen Wang[b], Keju Chen[b], Qingquan Zhu[b] and Guang He*[ab]

[a]Tianjin Key Laboratory of Advanced Functional Porous Materials, Institute for New Energy Materials and Low-Carbon Technologies, School of Materials Science and Engineering, Tianjin University of Technology, Tianjin 300384, P. R. China.

[b]Central Research Institute, Tianneng Co. LTD, Huzhou 313100, China.

Correspondence: heguang@tjut.edu.cn

Experimental Section

Material synthesis: $Li_{92.5}Cu_5Ag_{2.5}$ alloy foil is prepared by melting and two-step rolling. Firstly, Li-Cu alloy was prepared. The copper foil was put into molten lithium, heated continuously at 300 °C and stirred for 3 h with a stirrer. The prepared Li-Cu alloy is naturally cooled in a glove box filled with argon. The atomic content of Cu in Li-Cu composite was varied among 2 at%, 5 at%, 8 at% and 10 at%. The Li-Cu foils with different thicknesses can be obtained by adjusting the spacing between the two rollers of the rolling machine. The Li-Cu alloy foil and 1 μm thick Ag foil are rolled together by rolling machine again. Li and Ag have spontaneous reaction, and the alloying reaction is accelerated by low temperature heating (100°C).

Physical characterization: XRD characterization of alloy anodes were performed by Rigaku MiniFlex 600 with Cu Karadiaton. The surface morphology and the thickness of alloy anodes were characterized by SEM (Quanta FEG250 and FEI Verios 460L). Deposition process of lithium metal on the $Li_{92.5}Cu_5Ag_{2.5}$ and Li foil were observed using in situ optical microscopy (Keyence VHX-950F). The thickness of alloy foils with different areal capacities were also obtained by this microscopy.

Electrochemical evaluation: The Li foil, Li-Cu foils, and $Li_{92.5}Cu_5Ag_{2.5}$ were assembled in CR2032-type coins cells with Celgard separator. The electrolyte was 1.0 M LiTFSI in a 1:1 volume ratio mixture of DOL and DME with 3 wt% $LiNO_3$ and 1.0 M $LiPF_6$ in EC and DEC with a volume ratio of 1:1. The date of symmetric and full cells was collected on a LAND-CT 2001A multichannel battery cyclers at room temperature. Electrochemical impedance spectroscopy (EIS) was measured on the electrochemical workstation CHI760D (Tianjin, China).

SUPPLEMENTARY FIGURES

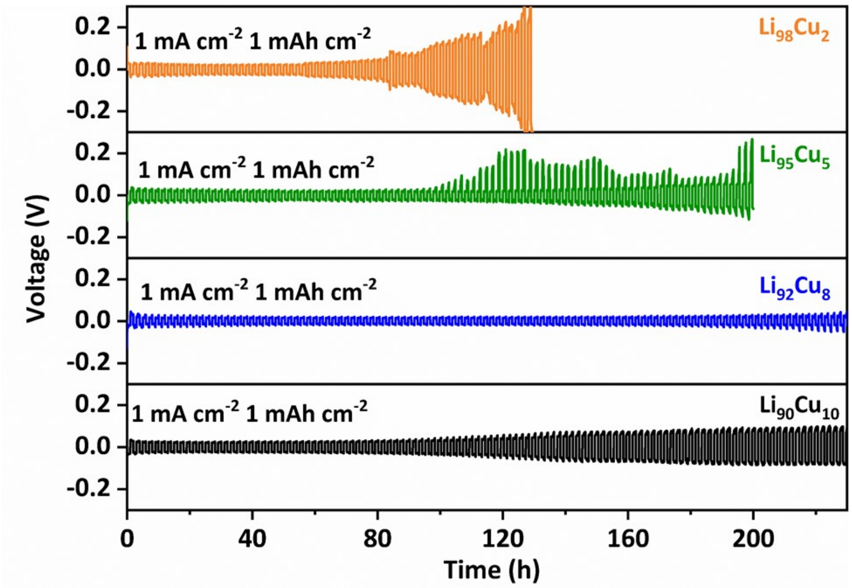

Fig. S1 Cycle performances of the symmetrical cells for Li-Cu electrodes with different Cu atomic contents at 1 mA cm^{-2}.

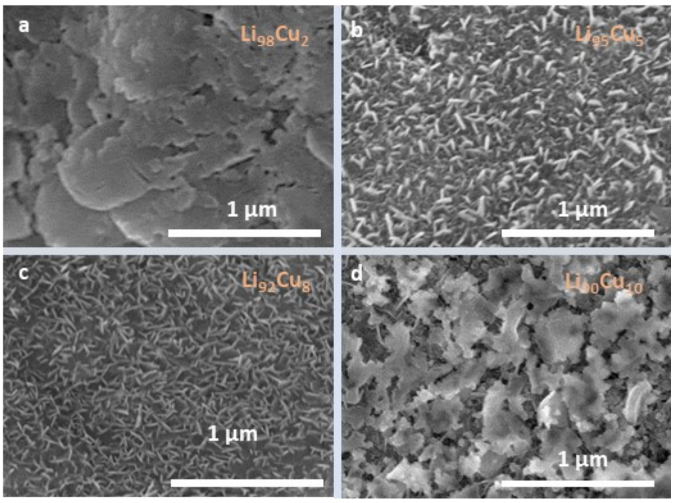

Fig. S2 SEM images of Li-Cu foil in different Cu content of (a) 2 at%, (b) 5 at%, (c) 8 at%, (d) 10 at% at stripping rate of 1 mA cm^{-2} for 2 mAh cm^{-2}.

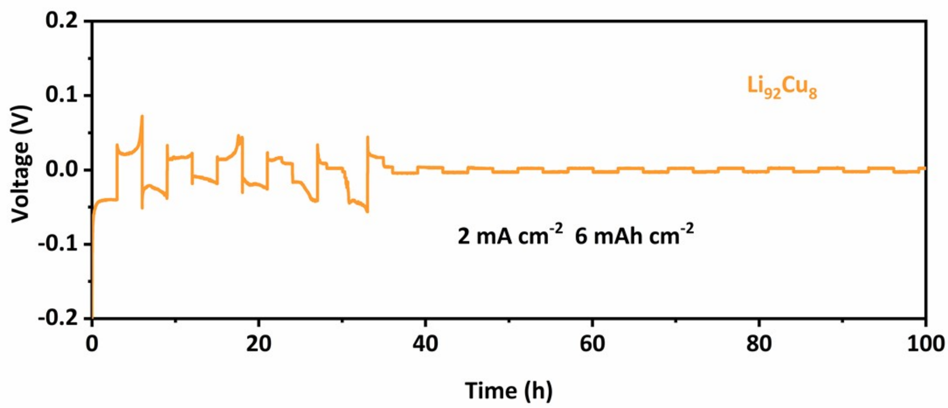

Fig. S3 Voltage-time curves of $Li_{92}Cu_8$ symmetric cells at 2 mA cm^{-2} with a Li striping/plating capacity of 6 mAh cm^{-2}.

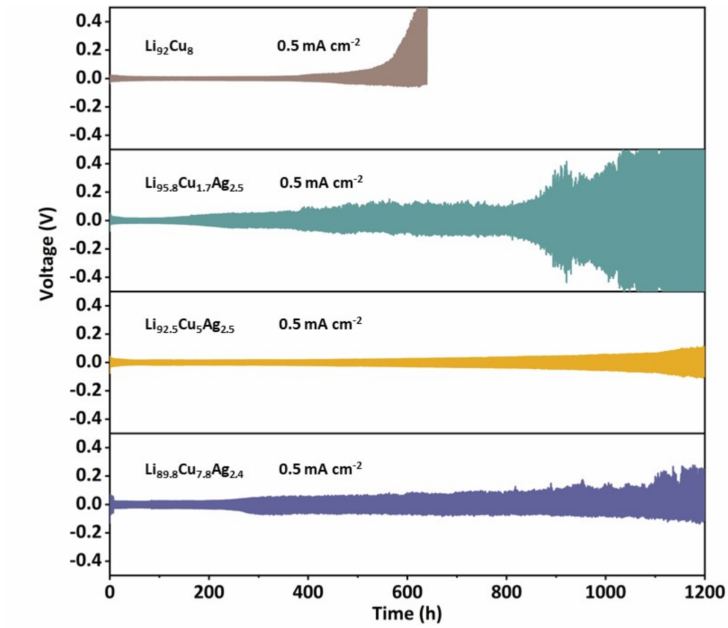

Fig. S4 Performance comparison of Li-Cu-Ag ternary alloy anodes with different atomic ratios in symmetric cells.

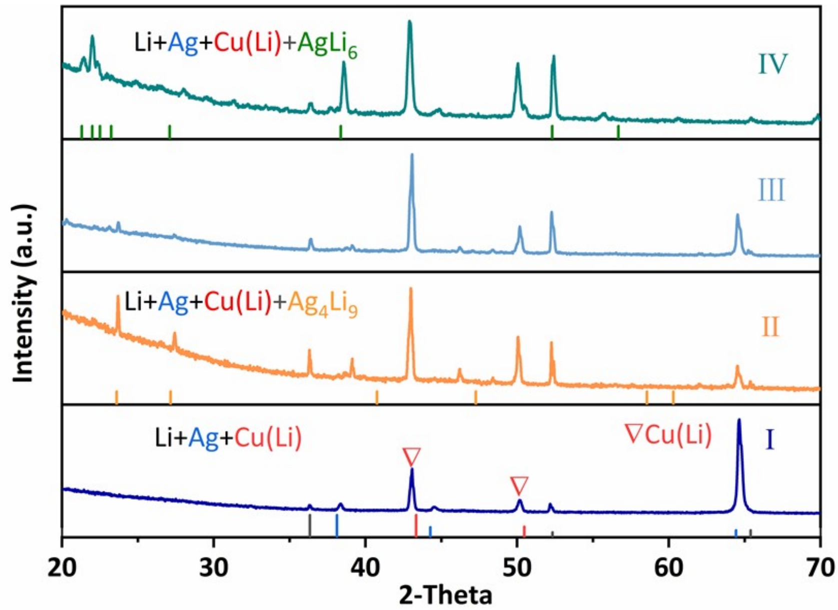

Fig. S5 Corresponding XRD patterns of $Li_{92.5}Cu_5Ag_{2.5}$ foil in different heating time.

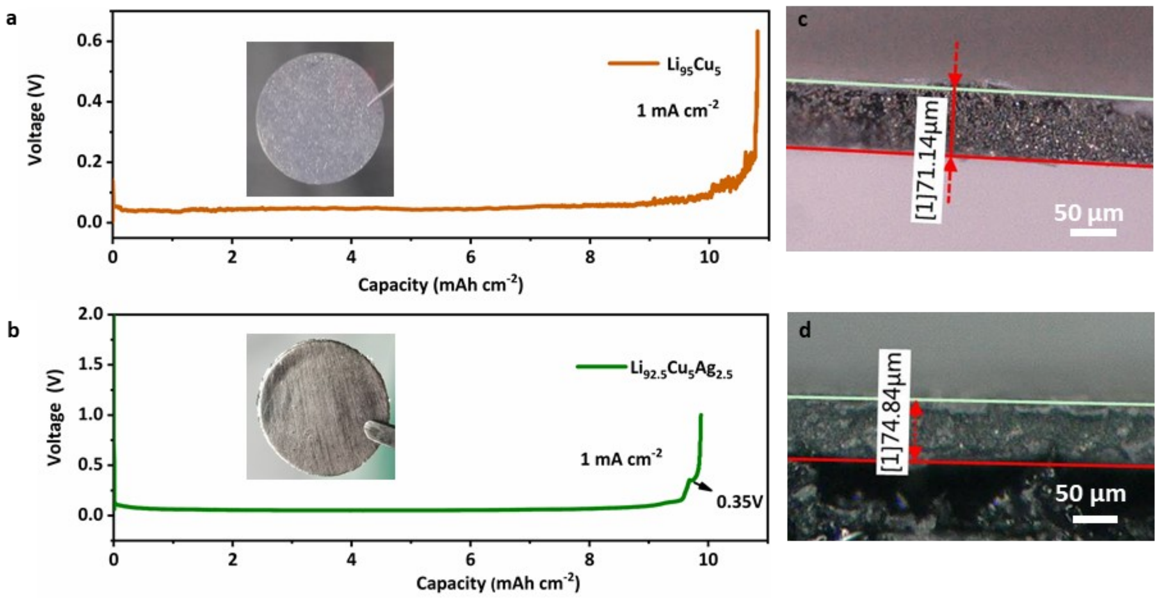

Fig. S6 Voltage profiles of delithiation on the $Li_{95}Cu_5$ anode (a) and $Li_{92.5}Cu_5Ag_{2.5}$ anode (b) at 1 mA cm^{-2} to a cut-off voltage of 1V. Optical microscopy images of the cross section of $Li_{95}Cu_5$ foil (c) and $Li_{92.5}Cu_5Ag_{2.5}$ foil (d). The areal capacity of the $Li_{92.5}Cu_5Ag_{2.5}$ is about 10 mAh cm^{-2} and its thickness 74 µm.

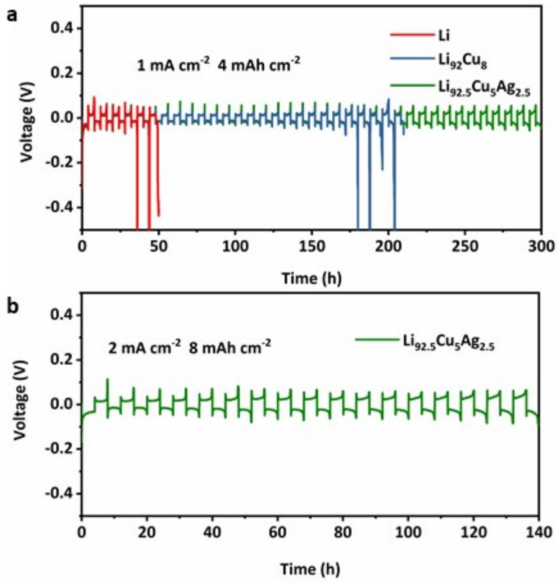

Fig. S7 Voltage-time curves of $Li_{92.5}Cu_5Ag_{2.5}$ symmetric cells at 1 mA cm^{-2} with a Li striping/plating capacity of 4 mAh cm^{-2} (a) and 2 mA cm^{-2} with a capacity of 8 mAh cm^{-2}(b).

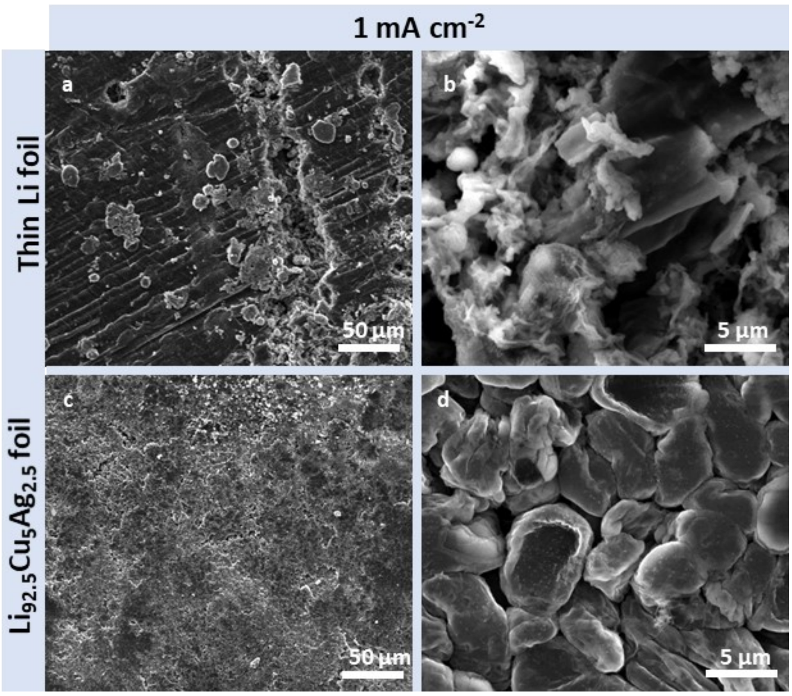

Fig. S8 SEM images of anode morphology after 20 cycles at 1 mA cm^{-2} in Li anode (a-b) and $Li_{92.5}Cu_5Ag_{2.5}$ anode (c-d) symmetrical cells.

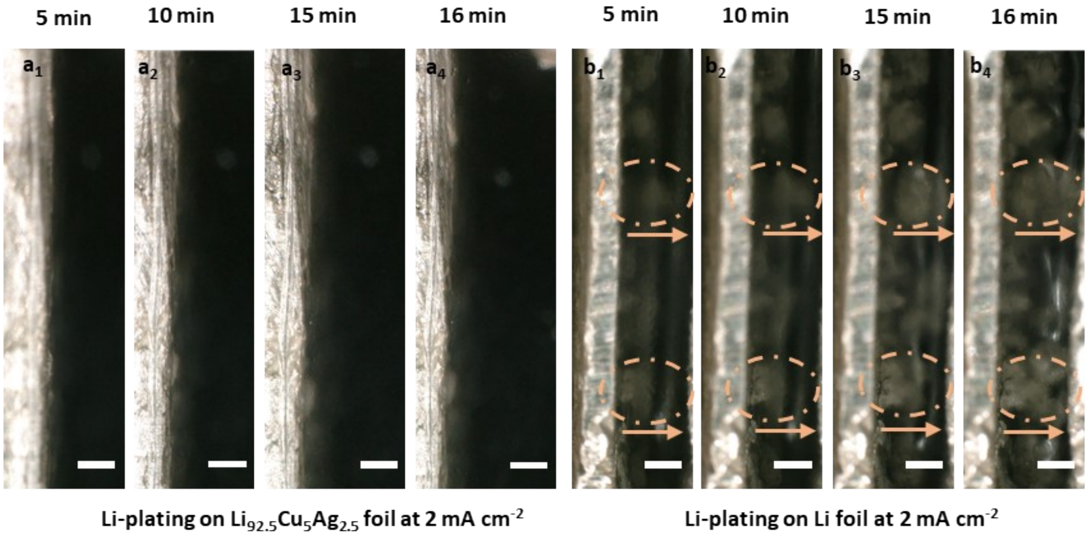

Fig. S9 In situ optical microscopy images of the cross section of the $Li_{92.5}Cu_5Ag_{2.5}$ electrode (a_1-a_4) and Li electrode (b_1-b_4).

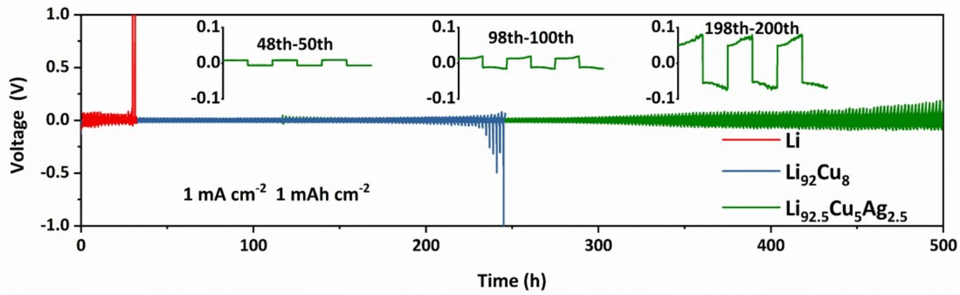

Fig. S10 Voltage profiles of three symmetric cells with a capacity of 1 mAh cm^{-2} at 1 mA cm^{-2}.

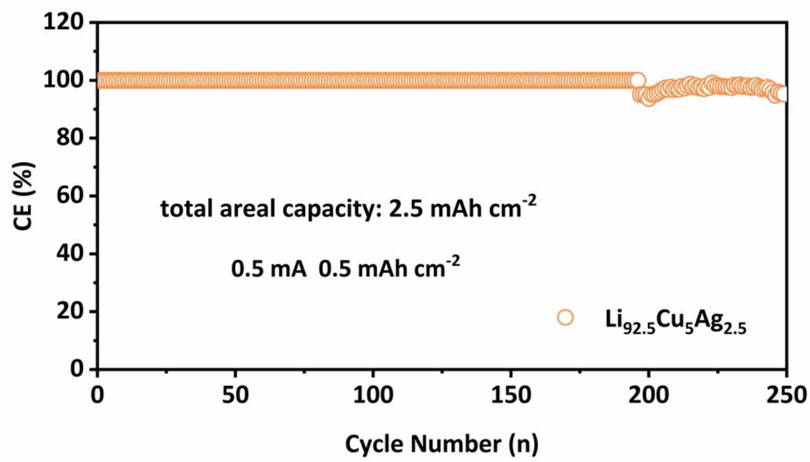

Fig. S11 The CE of ultrathin $Li_{92.5}Cu_5Ag_{2.5}$ (2.5 mAh cm^{-2}) foil with a cell configuration of Li|$Li_{92.5}Cu_5Ag_{2.5}$.

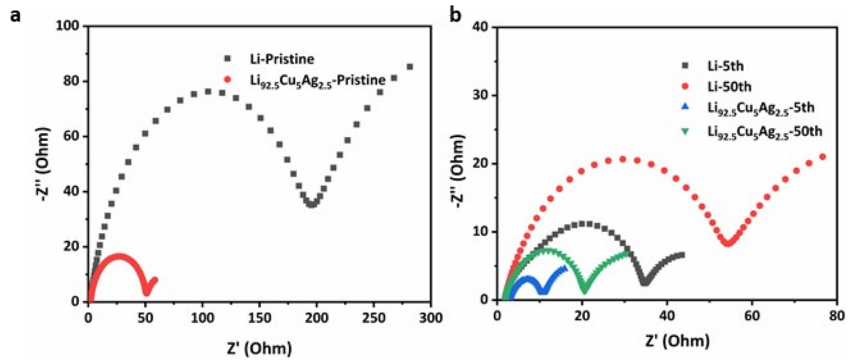

Fig. S12 EIS Profiles at 0th, 5th and 50th cycles of Li|Li and $Li_{92.5}Cu_5Ag_{2.5}$|$Li_{92.5}Cu_5Ag_{2.5}$ symmetrical cells.

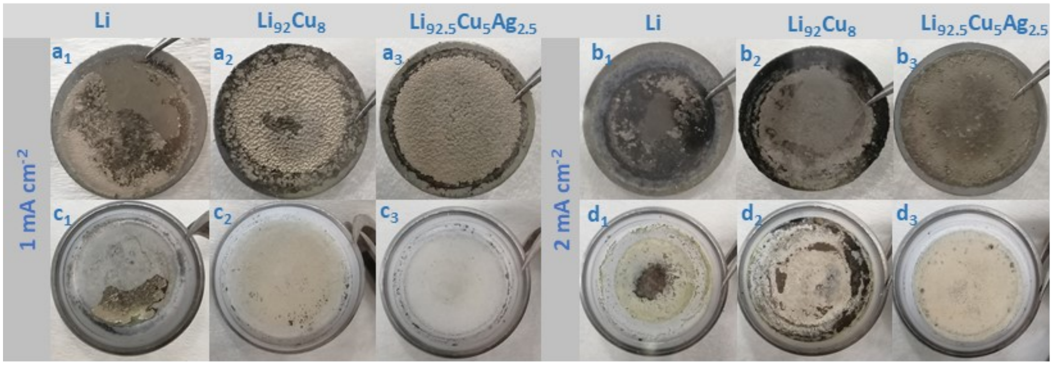

Fig. S13 The optical photograph of Li, $Li_{92}Cu_8$ and $Li_{92.5}Cu_5Ag_{2.5}$ foil in symmetric cells after cycling. Morphology of anodes at 1 mA cm^{-2}(a_1-a_3) and 2 mA cm^{-2}(b_1-b_3). Morphology of the separator at 1 mA cm^{-2}(c_1-c_3) and 2 mA cm^{-2}(d_1-d_3).

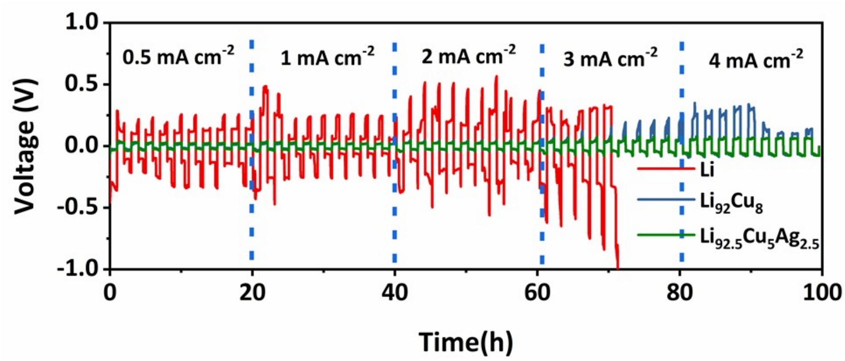

Fig. S14 Voltage–time curves of three symmetric cells at varied current densities.

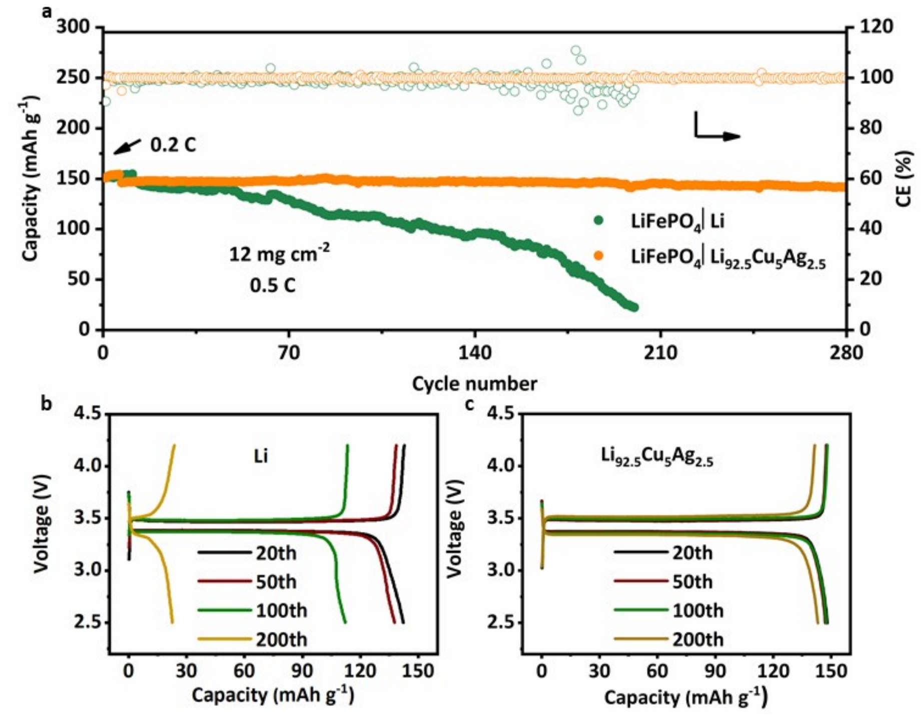

Fig. S15 (a) Cycling performance of $LiFePO_4$|Li and $LiFePO_4$|$Li_{92.5}Cu_5Ag_{2.5}$ full cells with $LiFePO_4$ mass loading of 12 mg cm^{-2} at 0.5 C; The voltage-capacity curves of $LiFePO_4$|Li cell (b) and $LiFePO_4$|$Li_{92.5}Cu_5Ag_{2.5}$ cell (c) at different cycles.

SUPPLEMENTARY TABLE

Table S1. Summary of weight and thickness of Li-Cu and $Li_{92.5}Cu_5Ag_{2.5}$ foils.

Samples	element atomic ratio	Mass (mg)	Area (cm^{-2})	Areal Mass Loading (mg cm^{-2})	Thickness (μm)
$Li_{98}Cu_2$	Li:Cu=98:2	4.06	1.327	3.07	57
$Li_{95}Cu_5$	Li:Cu=95:5	5.08	1.327	3.83	71
$Li_{92}Cu_8$	Li:Cu=92:8	6.18	1.327	4.64	88
$Li_{90}Cu_{10}$	Li:Cu=90:10	7.01	1.327	5.27	95
$Li_{92.5}Cu_5Ag_{2.5}$	Li:Cu:Ag=92.5:5:2.5	6.51	1.327	4.90	74